Phase noise measurement of high-power fiber amplifiers

Hu Xiao (肖 虎)[1*], Xiaolin Wang (王小林)[1], Yanxing Ma (马阎星)[1], Bing He (何 兵)[2], Pu Zhou (周 朴)[1], Jun Zhou (周 军)[2], and Xiaojun Xu (许晓军)[1]**

[1]*College of Opticelectric Science and Engineering, National University of Defense Technology, Changsha 410073, China*

[2]*Shanghai Institute of Optics and Fine Mechanics, Chinese Academy of Sciences, Shanghai 201800, China*

[*]*Corresponding author: xhwise@163.com;* [**]*corresponding author: zhoupu203@163.com*

Received October 18, 2010; accepted December 7, 2010; posted online March 28, 2011

We measure the phase fluctuation in a high-power fiber amplifier using a multi-dithering technique. Its fluctuation property is qualitatively analyzed by the power spectral density and integrated spectral density. Low frequency fluctuations caused by the environment are dominant in the phase fluctuations in an amplifier, whereas the high frequency components related to laser power affect the control bandwidth. The bandwidth requirement of the active phase-locking is calculated to be 300 Hz, 670 Hz, 1.6 kHz, and 3.9 kHz under the output power of 25, 55, 125, and 180 W, respectively. The approximately linear relationship between the control bandwidth and laser power needs to be further investigated.

OCIS codes: 060.2320, 140.3290, 140.3510.

doi: 10.3788/COL201109.041404.

Coherent beam combining has demonstrated to have the potential to solve the power limitation of a single fiber and obtain high power and high quality beams at the same time[1−7]. Coherent beam combining is implemented by phase locking, which forces all beams of an array to operate with the same phase; thus, when the beams overlap, the electric fields add constructive interference[1]. The active phase locking method based on master oscillator power amplifying (MOPA) structure is an effective approach to achieve this. To date, four-beam hundred-watt level fiber laser[8] and two-beam kilowatt level slab laser[9] coherent combinations are both achieved using this approach. In active phase locking, the combining result depends on whether the phase difference between beams of an array, which is also called phase fluctuation or phase noise, can be efficiently eliminated. Phase noise can be caused by pump beams or experimental environment factors such as mechanical oscillation, acoustic source, cooling fans, etc.[10,11] In previous work, phase fluctuations of 10-, 30-, and 260-W fiber amplifiers have been measured and characterized by Augst *et al.*[4,12] and Jones *et al.*[13] using heterodyne detection. Augst *et al.* also analyzed the effect of environmental elements on phase fluctuation. However, the dominant components of phase fluctuation and the bandwidth for phase locking at different power levels still need to be investigated.

In this letter, we measure the phase noise of a high-power amplifier. A four-stage end-pumped fiber amplifier is built. Phase fluctuations under different output power levels are measured using the multi-dithering technique. The phase fluctuations are characterized by computing the spectral density and structure function. The control bandwidths of different output levels are also calculated.

A schematic of the experimental setup for measuring phase fluctuation is shown in Fig. 1. The output power of a 1064-nm, linearly polarized, single-longitude-mode commercial fiber laser with a linewidth of about 10 MHz is pre-amplified by an end-pumped Yb-doped fiber (YDF) amplifier to attain 30 mW output and then split into two channels. One channel denoted as the reference beam is fused to a pig-tailed $LiNbO_3$ phase modulator and sent to a fiber collimator to form a collimated laser beam into free space. The other channel is also fused to a pig-tailed $LiNbO_3$ phase modulator and used to seed the four-stage YDF amplifier chain. The first three amplification stages of the chain are end-pumped amplifiers in an all-fiber configuration, and their maximum outputs are 100 mW, 1 W, and 30 W, respectively. The final power scaling amplifier is based on a bulk optics configuration and pumped by a 500-W collimated laser diode centered at 976 nm. The end of the output fiber is 8° cleaved to suppress parasitic oscillation. A high transmittance (HT) mirror is placed behind the output end of the power scaling amplifier. A small part of the output laser reflected by the HT mirror is coupled into a single-mode fiber through a focusing lens and transmitted to a collimator. The collimated beam array is sent to free space through the collimators. A 50:50 splitter mirror splits the collimated beam into two parts. After the splitter, one-half of the beam array is sent to a focusing lens that projects the central lobe of the far field onto a pinhole detector; a photodetector is located immediately behind the pinhole. Due to the difficulty of ensuring that the two beams are exactly parallel but with a small angle, the phase of the two beams varies with the position of the pinhole plane. Thus, the width of the pinhole is set to be 50% of the main lobe of the far-field pattern to reduce the phase difference caused by the position. The detected optical energy is shared by the oscilloscope and the controller, which drive the phase modulators. The other part of the beam array is sent to an infrared camera located at the focal plane of the lens to diagnose the far-field interference pattern. Isolators are used in every stage of the amplifiers to prevent backward beam. The last two stages are water cooled.

In this experiment, only one phase modulator (PM1) is used. PM1 is modulated at a radio frequency using a commercial lock-in amplifier. The phase noise is actually the relative optical phase difference between the reference and the amplified beams. The phase noise is measured using the multi-dithering technique. The theory of multi-dithering has been presented in detail in Ref.

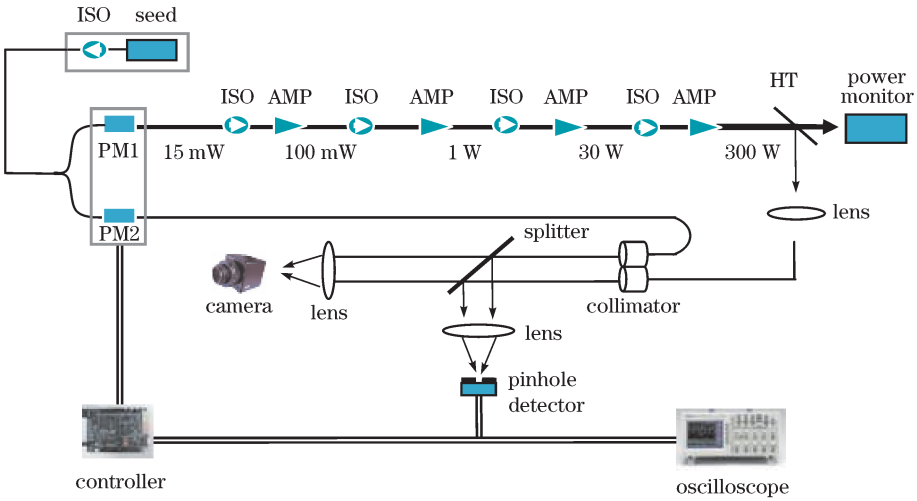

Fig. 1. Experimental setup. AMP: amplifier; ISO: isolator; PM1, PM2: phase modulators; HT: high transmittance mirror.

[14] and is only briefly reviewed here.

We use $E_u(t)$ and $E_l(t)$ to denote the optical fields of the reference beam and the amplified beam, respectively, which can be expressed as

$$E_u(t) = E_{u0}\cos(\omega t + \varphi_u), \tag{1}$$

$$E_l(t) = E_{l0}\cos(\omega t + \varphi_l + \beta_l \sin(\omega_l t)), \tag{2}$$

where E_{u0} and E_{l0} are the field amplitudes for the two channels, ϕ_u and ϕ_l are optical phases, β_l and ω_l are the amplitude and frequency of phase modulation for the amplified beam, respectively, and ω represents the laser frequency. The optical intensity of the overlapped field at the pinhole can be expressed as

$$\begin{aligned} I(t) &= \sqrt{\frac{\varepsilon_0}{\mu_0}}\left[E_u(t) + E_l(t)\right]^2 \\ &= \sqrt{\frac{\varepsilon_0}{\mu_0}}\left[E_u^2(t) + E_l^2(t) + 2E_u(t)E_l(t)\right]. \end{aligned} \tag{3}$$

The output current of the photodetector can be expressed as

$$i_{\mathrm{PD}}(t) = R_{\mathrm{PD}} \cdot A \cdot I(t), \tag{4}$$

where R_{PD} represents the responsivity of the photodetector, and A is the photodetector area. The phase fluctuation signal can be given by

$$S = \frac{1}{\tau}\int_0^{\tau} i_{\mathrm{PD}}(t) \cdot \sin(\omega_l t)\mathrm{d}t, \tag{5}$$

where τ represents the integration time. When τ is short enough,

$$S = R_{\mathrm{PD}} A \sqrt{\frac{\varepsilon_0}{\mu_0}} J_1(\beta_l) E_{u0} E_{l0} \sin(\varphi_u - \varphi_l), \tag{6}$$

where J_1 represents the first order Bessel function, and $\sin(\varphi_u - \varphi_l)$ is the sinusoidal value of the phase difference between the two beams. Thus, the phase difference can be calculated from S, which is proportional to $\sin(\varphi_u - \varphi_l)$.

In this experiment, phase fluctuation was measured at four different output power levels. The output powers of the amplified laser beam were 25, 55, 125, and 180 W, respectively. In fact, the output power can reach 300 W if the spectral width of the seed laser is broad enough to suppress stimulated Brillouin Scattering (SBS). Nevertheless, the seed laser used here operated in the single longitude mode and could lead to dramatic SBS. Hence, we did not achieve an output that high owing to the risk of optical damage. The time series of the amplifier's phase fluctuation under different laser powers were recorded using the oscilloscope, as shown in Fig. 2. The high frequency components increase with the rise of output power, which corresponds to an increase in pump power. The negative bias to phase fluctuations exists in Fig. 2. This is due to the initial optical path difference between the two optical channels in our experimental setup; it has little effect on phase fluctuation characteristics.

Performing a fast Fourier transform on the phase fluctuation data shows the spectral characteristics of phase noise in detail (Fig. 3). In Fig. 3, with the output

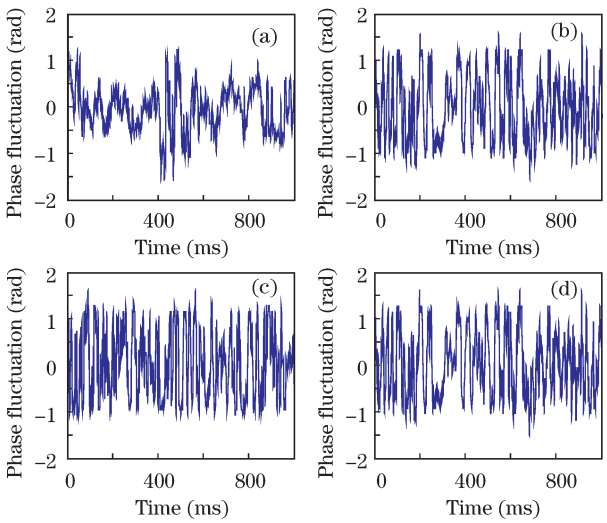

Fig. 2. Amplifier phase fluctuation at different output powers: (a) 25 W, (b) 55 W, (c) 125 W, (d) 180 W.

power increasing, the high frequency components become stronger, whereas the lower frequency components become weaker. Figure 4 shows the integrated spectral density, which represents the cumulative root-mean-square (RMS) phase variation of all frequencies below the frequency of interest. It is expressed as follows[13,15]:

$$I_n(f) = \left(\int_0^f S^2(\nu)\mathrm{d}\nu\right)^{1/2} \Big/ \left(\int_0^f S^2(\nu)\mathrm{d}\nu\right)^{1/2}, \quad (7)$$

where $S(\nu)$ is the spectral density of phase fluctuation. Figure 4 shows that the weight of the frequency components below 10 Hz falls from 50% to approximately 35% when the output power increases from 25 to 180 W. This means that the weight of the high frequency components increases as the output power increases, which could be caused by pump power fluctuations. The instability of laser diode current can lead to pump power fluctuations, which, as a result, disturbs the steady temperature distribution. Thus, the refractive index of the fiber core, which is dependent on temperature and stress, changes rapidly and finally leads to the fluctuating phase difference between the two optical channels. The fluctuation amplitude and frequency of laser diode current may increase with the pump power, and thus the weight of the high frequency components increases with the pump power.

Note that the low frequency components mainly caused by environmental elements still dominate even when the output power is as high as 180 W. Based on Figs. 3 and 4, the dominant phase fluctuation of our experimental

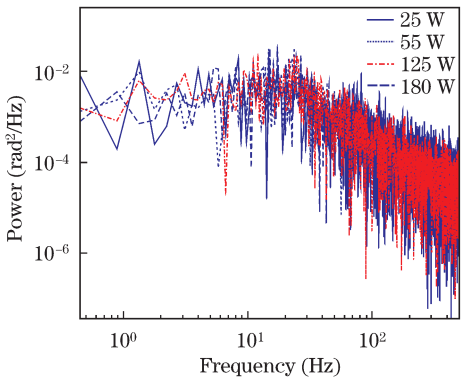

Fig. 3. Phase fluctuation spectral density.

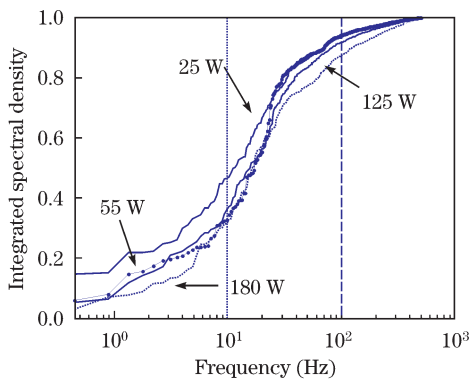

Fig. 4. Integrated phase fluctuation spectral density.

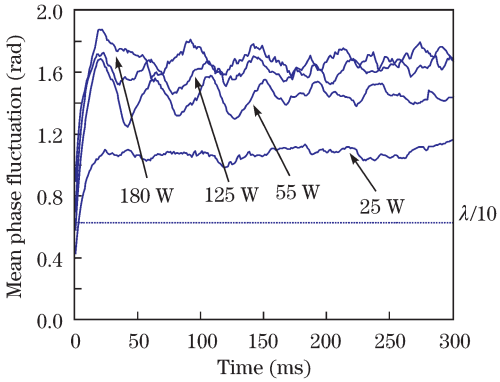

Fig. 5. Structure function of the phase fluctuation under different output powers.

setup is the environmental noise, which is below 100 Hz. The pump power affects the high frequency components but cannot dominate the phase fluctuation.

As shown in Refs. [13] and [14], although spectral density can represent the frequency component in a qualitative way, the control bandwidth requirement estimated from it is usually not adequate. The reason is that the spectral density is a plot of RMS values; non-Gaussian and nonstationary noise will appear at a greatly reduced level[12]. Compared with the spectral density, structure function can quantify the level of phase fluctuation, characterizing the average phase deviation in the noise component after a time τ[12,13]. The structure function is defined as[15]

$$\mathrm{SF} = \langle|\varphi(t+\tau) - \varphi(t)|\rangle\,. \quad (8)$$

This quantity gives useful insights into the rate at which phase fluctuations accumulate in time. The structure function curves of the four output powers are calculated, as shown in Fig. 5. There is a clear indication of large low frequency components in the range of tens of hertz. The dashed line in Fig. 5 denotes a suggested phase tolerance ($\lambda/10$) for practical phase correction. In Fig. 5, the time periods for phase fluctuations over $\lambda/10$ under the powers of 25, 55, 125, and 180 W are about 3.3, 1.5, 0.9, and 0.6 ms, respectively. Thus, our experimental setup estimates that the control bandwidth for phase locking should be at least 300 Hz, 670 Hz, 1.6 kHz, and 3.9 kHz, respectively, at these four different output levels. The level of phase fluctuation is much lower than that in Ref. [15], whose phase fluctuation is mainly caused by optic-thermo effects in a strongly pumped fiber amplifier. In summary, although environmental elements dominate, the amplitude of the fast fluctuating components has an effect on phase locking. Thus, the control bandwidths should be broadened as the laser power increases.

In conclusion, we have measured the phase fluctuations of a high-power amplifier under the output powers of 25, 55, 125, and 180 W. The phase fluctuations are characterized by the power spectral density and the integrated spectral density. The results show that high frequency components weigh more as the output power increases, but low frequency noise below 100 Hz still dominates. In our experiment, the phase noise is mainly environmental noise. Estimated from the structure function, the minimum bandwidth requirements of the active phase-locking

system are 300 Hz, 670 Hz, 1.6 kHz, and 3.9 kHz, respectively, for the four output powers. Our experiment has demonstrated that the environmental elements causing low frequency fluctuations are dominant components in the phase fluctuations of an amplifier, whereas the high frequency components of laser power affect the control bandwidth and combining results.

The authors are grateful to Mr. Chi Liu, Mr. Yuhao Xue, and Mr. Zhen Li for their enthusiasm in the study and their generous assistance in providing the fiber amplifiers.

References

1. T. Y. Fan, IEEE J. Sel. Top. Quantum Electron. **11,** 567 (2005).
2. M. A. Vorontsov, Proc. SPIE **5895,** 589501 (2005).
3. W. Wang, B. He, J. Zhou, Q. Lou, X. Liu, F. Zhang, S. Zhang, and H. Xu, High Power Laser and Particle Beams (in Chinese) **20,** 1802 (2008).
4. S. J. Augst, T. Y. Fan, and A. Sanchez, Opt. Lett. **29,** 474 (2004).
5. P. Zhou, "Study on coherent beam combination technology of fiber lasers" (in Chinese) PhD. Thesis (National University of Defense Technology, Changsha, 2009).
6. P. Zhou, Z. Liu, and X. Xu, Chinese J. Lasers (in Chinese) **36,** 276 (2009).
7. Z. Liu, J. Hou, X. Xu, Y. Feng, P. Zhou, Z. Chen, Y. Ma, X. Wang, B. Lei, and J. Cao, Chinese J. Lasers (in Chinese) **36,** 2773 (2009).
8. M. Wickham, J. Anderegg, S. Brosnan, E. Cheung, P. Epp, D. Hammons, H. Komine, and M. Weber, Proc. SPIE **6102,** 61020U (2006).
9. G. D. Goodno, H. Komine, S. J. McNaught, S. B. Weiss, S. Redmond, W. Long, R. Simpson, E. C. Cheung, D. Howland, P. Epp, M. Weber, M. McClellan, J. Sollee, and H. Lajeyan, Opt. Lett. **31,** 1247 (2006).
10. M. K. Davis, M. J. F. Digonnet, and R. H. Pantell, J. Lightwave Technol. **16,** 1013 (1998).
11. Z. Chen, J. Hou, and Z. Jiang, Chin. Opt. Lett. **5,** 178 (2007).
12. S. J. Augst, J. K. Ranka, T. Y. Fan, and A. Sanchez, J. Opt. Soc. Am. B **24,** 1707 (2007).
13. D. C. Jones, C. D. Stacey, and A. M. Scott, Opt. Lett. **32,** 466 (2007).
14. T. M. Shay, V. Benham, J. T. Baker, A. D. Sanchez, D. Pilkington, and C. A. Lu, IEEE J. Sel. Top. Quantum Electron. **13,** 480 (2007).
15. P. Zhou, X. Wang, Y. Ma, J. Leng, H. Ma, J. Wang, X. Xu, and Z. Liu, J. Phys. B: At. Mol. Opt. Phys. **42,** 195401 (2009).